Tetrahedron 67 (2011) 2911–2915

Contents lists available at ScienceDirect

Tetrahedron

journal homepage: www.elsevier.com/locate/tet

Synthesis, structures and inclusion properties of tetranaphthalides: new macrocyclic clathrate hosts

Koichi Tanaka [a,*], Kyosuke Hori [a], Asuka Masumoto [a], Ryuichi Arakawa [a], Mino R. Caira [b,*]

[a] Department of Chemistry and Materials Engineering, Faculty of Chemistry, Materials and Bioengineering, Kansai University, Suita, Osaka 564-8680, Japan
[b] Department of Chemistry, University of Cape Town, Rondebosch 7701, South Africa

ARTICLE INFO

Article history:
Received 5 December 2010
Received in revised form 18 February 2011
Accepted 21 February 2011
Available online 26 February 2011

ABSTRACT

Novel tetranaphthalide host compounds **3** and **4** bearing isomeric naphthalene moieties have been synthesized and their inclusion properties were investigated. These host compounds enclathrated several kinds of ketones, cyclic ethers, amides, sulfoxides and aromatic compounds. The structures of two representative inclusion compounds containing different host molecules and a common guest (dimethyl sulfoxide) were investigated by X-ray diffraction to determine the nature of guest inclusion and to rationalize their distinctly different thermal decomposition profiles.

1. Introduction

There has been increasing interest in host/guest inclusion compounds because of their potential applications, such as separation of isomeric compounds,[1] optical resolution of racemates,[2] reaction medium of included molecules[3] and sensor materials.[4] Macrocyclic host compounds have been studied intensively during the last few decades.[5] Calixarene is one of the useful host molecules in supramolecular systems and the subtype of heteroatom-bridged calixarene compounds including oxygen,[6] sulfur,[7] nitrogen[8] and amide[9] has been developed. Recently, we reported the synthesis, crystal structure and inclusion properties of novel ester bond bridged calixarene analogues, tetra- and hexa-salicylide hosts (**1** and **2**).[10] The tetrasalicylide hosts having a 5-substituted halogen atom on the aromatic ring form organogels with several kinds of organic solvents, whereas the hexa-salicylide hosts are prone to include several organic solvent molecules in the solid state. With a view to exploring the potential host properties of isologues of tetra- and hexa-salicylides, we have examined the cyclocondensation reaction of some hydroxynaphthoic acid derivatives as valuable precursors bearing larger aromatic components. Here, we report the synthesis and inclusion properties of novel tetranaphthalide host compounds **3a**,**b** and **4**, as well as two representative crystal structures.

2. Results and discussion

2.1. Synthesis of tetranaphthalides and their inclusion properties

The tetranaphthalides were synthesized by a cyclization reaction of the corresponding hydroxynaphthoic acid derivatives in toluene in the presence of $POCl_3$. For example, a mixture of 3-hydroxy-2-naphthoic acid **5a** and $POCl_3$ was heated in toluene under reflux for 6 h. After cooling the reaction mixture to room temperature, the crystals deposited were separated by filtration and washed with water and aq $NaHCO_3$ solution and filtered. The crystalline solid was collected and purified by silica gel column chromatography to give **3a** in 54% yield.

Similar treatment of 7-methoxy-3-hydroxy-2-naphthoic acid **5b** and 1-hydroxy-2-naphthoic acid **6** afforded corresponding tetranaphthalides **3b** and **4** in 48% and 23% yield, respectively. However, similar treatment of 2-hydroxy-1-naphthoic acid **7** gave only 2-naphthol **8** in 54% yield instead of the tetranaphthalide. This may be due to the severe steric repulsion between aromatic rings of the naphthalide.

A variety of organic solvents including cyclic ethers, cyclic and acyclic ketones, amides, sulfoxides and several kinds of aromatic compounds were used for the inclusion experiments (Table 1). The inclusion crystals were obtained by recrystallization of the tetranaphthalide from the respective guest solvents. The host/guest ratios were evaluated by TGA and ^1H NMR spectral integration. As shown in Table 1, tetranaphthalides **3a** and **3b** showed excellent inclusion ability and included all the guest solvents tested in Table 1. The host/guest stoichiometric ratios of 1:5 (guests: cyclohexanone, DMSO) and 1:4 (guests: diethylketone, aniline) are

* Corresponding authors. E-mail address: ktanaka@ipcku.kansai-u.ac.jp (K. Tanaka).

0040-4020/$ – see front matter © 2011 Elsevier Ltd. All rights reserved.
doi:10.1016/j.tet.2011.02.053

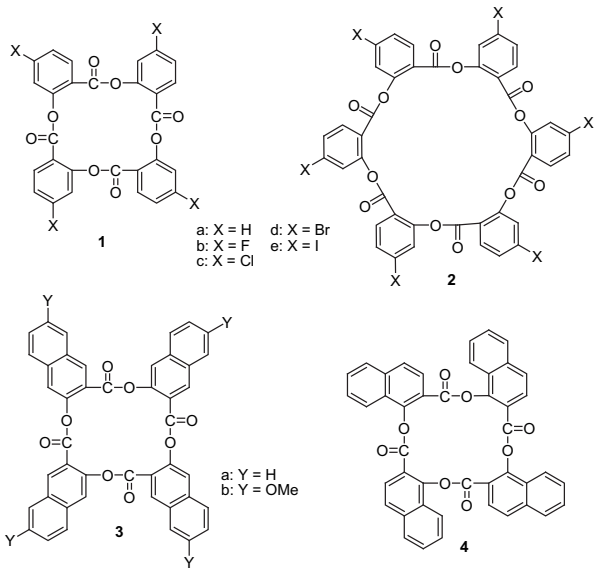

Table 1
Host/guest ratios and guest release temperatures of the inclusion crystals of **3a**, **3b** and **4**

Guest	**3a**	**3b**	**4**
Diethylketone	1:4[b] (84)[c]	2:3 (84)	—[a]
Cyclopentanone	2:3 (161)	1:1 (57)	1:1 (165)
Cyclohexanone	1:5 (102)	2:3 (76)	1:2 (137, 175)
1,4-Dioxane	2:3 (145)	1:1 (70)	2:3 (94, 138)
DMSO	1:5 (120)	1:2 (237)	1:2 (121)
DMF	1:2 (176)	1:2 (191, 212)	—
Pyridine	1:2 (65)	1:1 (64)	1:4 (89)
2-Methylpyridine	1:3 (122)	2:3 (124, 143)	1:1 (136)
3-Methylpyridine	1:3 (146)	1:2 (185)	1:1 (101)
4-Methylpyridine	1:1 (173)	1:2 (120, 146)	1:1 (163)
Benzene	1:2 (83)	1:1 (70)	1:1 (72)
Aniline	1:4 (169)	1:2 (118)	1:3 (103, 151)
Anisole	1:3 (127)	1:2 (69)	—
Chlorobenzene	1:2 (137)	1:1 (70)	—
Bromobenzene	1:3 (123, 162)	1:1 (72)	—
o-Dichlorobenzene	1:3 (126)	1:1 (68, 172)	1:2 (137, 147)
m-Dichlorobenzene	1:1 (185)	1:1 (78)	1:1 (139)
o-Xylene	1:3 (128)	2:1 (75)	1:1 (176)
m-Xylene	1:1 (184)	1:1 (60)	1:1 (157)
p-Xylene	1:2 (113, 152)	1:1 (72)	2:3 (106, 139)

[a] No inclusion complexation.
[b] Host/guest ratios were determined by TG and ^{1}H NMR spectroscopy.
[c] Guest release temperature (°C).

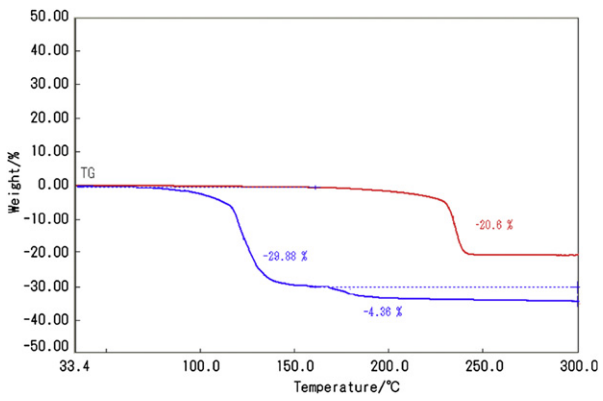

Fig. 1. TGA traces for the 1:5 DMSO complex of **3a** (blue line) and 1:2 DMSO complex of **3b** (red line).

exceptionally large, which indicates the high efficiency of guest accommodation by these host compounds. However, tetranaphthalide **4** showed relatively poor inclusion ability. This is attributable to the low symmetry of the molecular structure of **4**. As for the inclusion of DMSO, host **3b** showed higher guest release temperature (237 °C) than that of host **3a** and **4**. The thermogravimetric analysis (TGA) data for these complexes are shown in Fig. 1. Similar behaviour was observed for the inclusion of 3-methylpyridine.

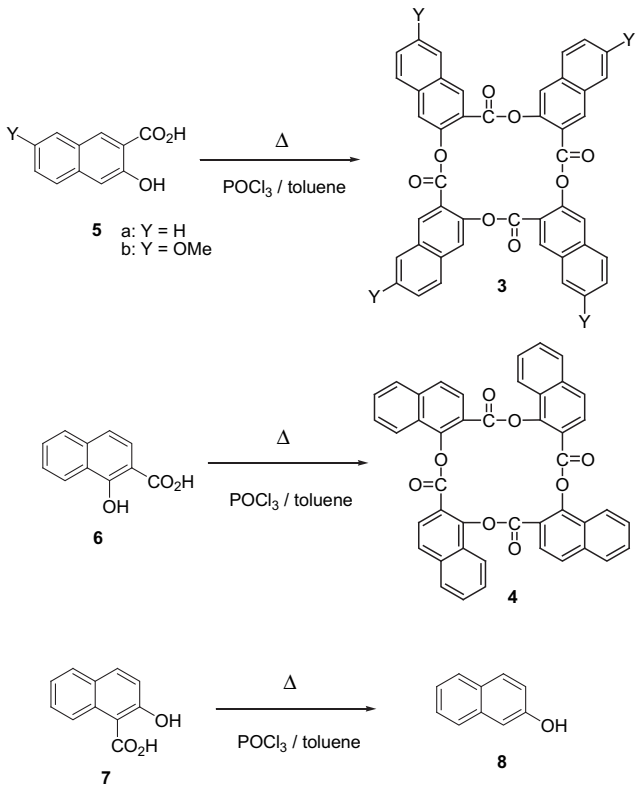

2.2. X-ray structural analyses

Table 2 lists crystal data and refinement parameters for the representative inclusion compounds **3a**·(DMSO)$_5$ and **3b**·(DMSO)$_2$, whose structures were investigated to establish the nature of common guest inclusion by the respective host molecules and to rationalize the significantly different thermal stabilities of these species (Fig. 1).

Table 2
Crystal data and refinement parameters for two representative inclusion compounds of host molecules **3a** and **3b**

	3a·(DMSO)$_5$	**3b**·(DMSO)$_2$
Formula	$C_{44}H_{24}O_8\cdot(C_2H_6OS)_5$	$C_{48}H_{32}O_{12}\cdot(C_2H_6OS)_2$
Formula weight	1071.27	956.99
Crystal system	Tetragonal	Tetragonal
Space group	$I4_1/a$	$I4_1/a$
a, Å	18.9747 (4)	13.9412 (19)
c, Å	14.6378 (4)	23.0660 (16)
V, Å^3	5270.2 (2)	4483.0 (9)
Z	4	4
T, K	113 (2)	100 (2)
λ, Å	0.71073 (Mo Kα)	0.71073 (Mo Kα)
R_1	0.0486	0.0437
wR_2	0.1151	0.1143
Goodness of fit	1.055	1.038

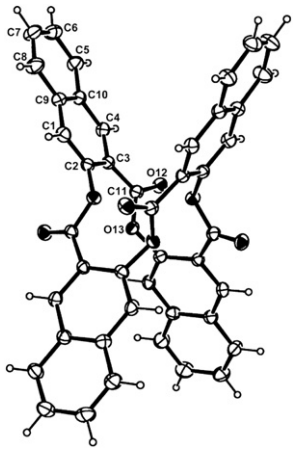

Fig. 2. ORTEP diagram of host **3a** in its inclusion compound with DMSO, showing the atomic numbering of the asymmetric unit and thermal ellipsoids drawn at the 50% probability level.

The molecule of tetranaphthalide **3a** (Fig. 2) is located on a fourfold inversion centre with the orientations of the four naphthalene residues alternating up and down, these residues being held together by *trans* ester linkages (representative torsion angle C3–C11–O13–C2^{i}=−174.2 (2)°, *i*=3/4−*y*, −1/4+*x*, 3/4−*z*). Furthermore, the conformation adopted by **3a** is that in which the four carbonyl groups are directed away from the inversion centre, ester oxygen atom O13 and its three symmetry-related counterparts forming a flattened tetrahedron at the centre of the molecule with O···Cg···O angles in the range 96.8–139.7° (where Cg is the centroid of the four ester O atoms). The closest O···O contact distance is 2.645 (1) Å. As concerns inclusion ability, an important parameter characterizing host molecule **3a** is the angle between two diad-related naphthalene rings, since this determines the size of guest or guest residue that may be accommodated within the V-shaped groove, which these planes define. For the conformation adopted by molecule **3a**, this angle is 54.8 (1)°.

In the asymmetric unit of **3a**·(DMSO)$_5$, there are two crystallographically independent DMSO molecules: one of these is located in a general position (multiplicity 16) while the other is disordered around a position of fourfold-inversion (-4) symmetry, with the oxygen atom on the C_2-axis passing through this point (accounting for four additional DMSO molecules per unit cell). The host/guest ratio is thus 4:20, or 1:5 (Table 1). The DMSO content is high owing to accommodation of solvent molecules both within the hosts' V-shaped clefts (disordered DMSO) and in the interstitial spaces between host molecules (ordered DMSO). Fig. 3 shows a single molecule of **3a** with its assembly of nearest-neighbour DMSO molecules.

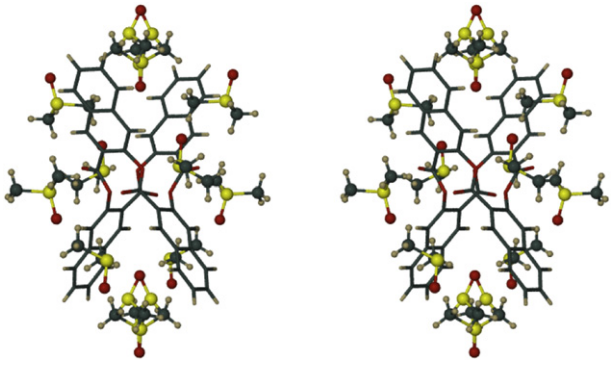

Fig. 3. Stereoview of a single molecule of host **3a** surrounded by DMSO molecules. The host molecule is represented in stick mode while the solvent molecules are shown in ball-and-stick representation.

In effect, the host surface is almost completely solvated by surrounding DMSO molecules. As a result, there are no direct host···host interactions. Instead, DMSO molecules act as bridges between neighbouring host molecules (Fig. 4). Thus, each naphthalene ring of host molecule **3a** engages in two C–H···O hydrogen bonds, the acceptors being oxygen atoms of inversion-related DMSO molecules. The result is a centrosymmetric ring motif, R (14), with C···O distances 3.356 (3) Å (C1–H1···O15) and 3.299 (3) Å (C7–H7···O15). There are no significant π-interactions between aromatic rings of neighbouring host molecules.

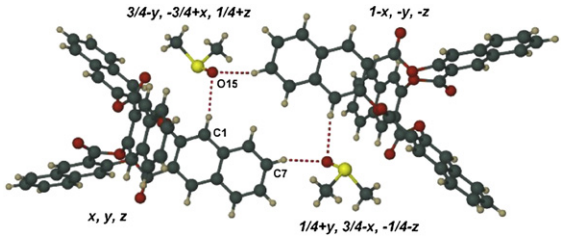

Fig. 4. Hydrogen bonded motif in **3a**·(DMSO)$_5$.

The distinctive two-step TGA mass loss observed on heating inclusion compound **3a**·(DMSO)$_5$ can be accounted for qualitatively and quantitatively on the basis of its crystal structure. As noted above, the included DMSO molecules occur in two distinct sets in a ratio of 4:1, those in general positions (16 per unit cell) and those arranged around the positions of fourfold-inversion symmety (4 per unit cell). Fig. 5 shows the arrangement of the DMSO molecules located in general positions. They generate a series of infinite spirals parallel to the crystal *c*-axis. Within a spiral, the DMSO molecules are in close contact.

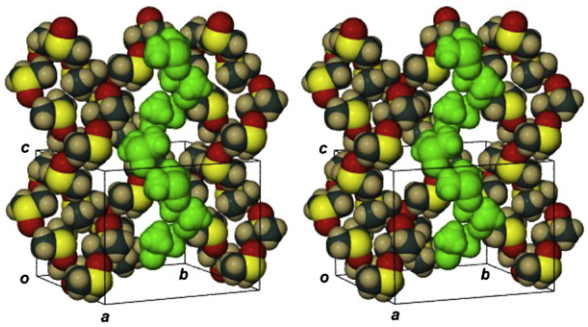

Fig. 5. Stereoview of the arrangement of DMSO molecules located in general positions in the unit cell. For clarity, a representative spiral is shown in green.

In contrast, DMSO molecules located around fourfold inversion axes are very efficiently encapsulated within the cavity formed by two abutting host molecules. In Fig. 6, one such representative

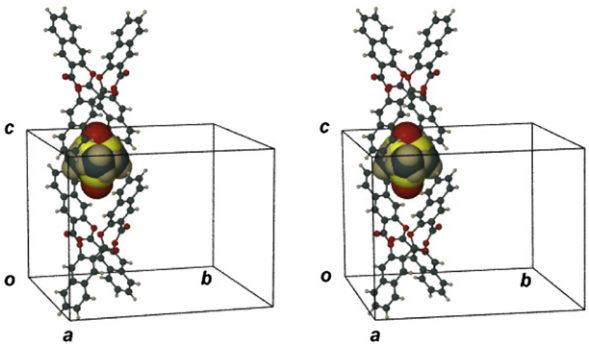

Fig. 6. Stereoview of a disordered DMSO molecule in **3a**·(DMSO)$_5$ enclathrated by two host molecules.

disordered molecule of DMSO (of four in the unit cell) is shown for simplicity.

Thus, on heating the inclusion compound **3a**·(DMSO)$_5$, it can be envisaged that the weakly bound DMSO molecules, arranged in continuous infinite spirals (Fig. 5), diffuse along the *z*-direction out of the crystal first (i.e., at relatively low temperature, ~120 °C), as shown in Fig. 1, accounting for an initial observed mass loss of ~30% (calcd for loss of four DMSO molecules per **3a**·(DMSO)$_5$ unit: 29.2%). This would be followed by the loss of the significantly more tightly bound DMSO molecules (Fig. 6) at considerably higher temperature (~170 °C), accounting for the observed second mass loss of ~5% (Fig. 1). The theoretical mass loss for the remaining DMSO molecule in **3a**·(DMSO)$_5$ is 7.3%.

The inclusion compound **3b**·(DMSO)$_2$ also crystallizes in the tetragonal space group $I4_1/a$ with the host molecule again located on a fourfold inversion centre (Fig. 7). However, relative to host **3a**, molecule **3b** adopts an inverted conformation, with the four carbonyl groups (C13═O14 and symmetry-related counterparts) now directed towards the centre of the host molecule while the four ester oxygen atoms (O15 and counterparts) are at the periphery.

The four carbonyl oxygen atoms are in a slightly distorted tetrahedral array (O···Cg···O angles in the range 102.9–112.9°, where Cg is the centroid) and the shortest O···O contact is 2.996 (1) Å. *trans* Ester linkages (C1–C13–O15–C2^{ii}=−170.1 (1)°, ii=5/4−*y*, 1/4+*x*, 1/4−*z*) are again responsible for holding the macrocycle together. A further consequence of the inverted conformation in **3b** is that the angle between diad-related naphthalene ring planes is 85.6 (1)°, i.e., considerably larger than that in **3a**, namely 54.8 (1)°. The distinctly different conformations of host molecules **3a** and **3b** are further contrasted in Fig. 8.

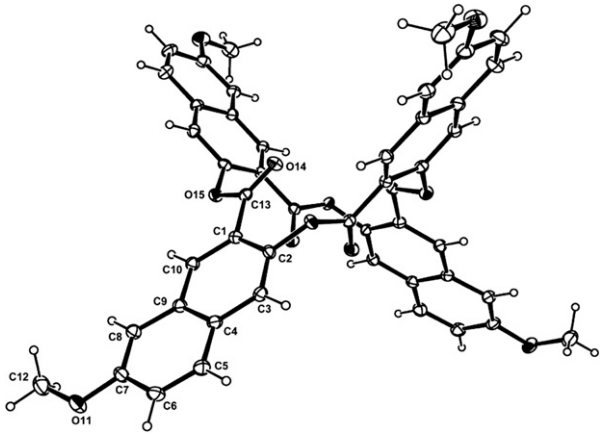

Fig. 7. ORTEP diagram of host **3b** in its inclusion compound with DMSO, showing atomic numbering of the asymmetric unit and thermal ellipsoids drawn at the 50% probability level.

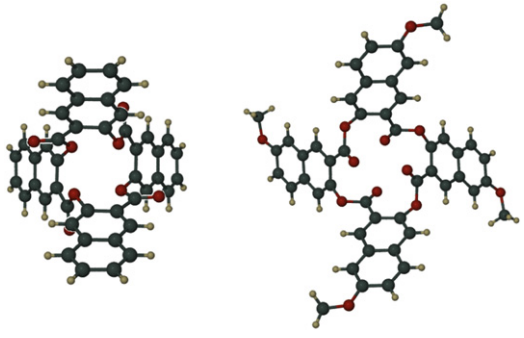

Fig. 8. Host molecules **3a** (left) and **3b** (right) viewed down their symmetry axes.

Neighbouring host molecules **3b** are tethered by bifurcated hydrogen bonds C5–H···O14^{iii} (iii=3/4−*y*, 1/4+*x*, 1/4+*z*) and C5–H···O15^{iv} (iv=−1/2+*x*, *y*, 1/2−*z*) with C···O distances of 3.397 (2) and 3.184 (2) Å, respectively.

The DMSO molecule in the inclusion compound **3b**·(DMSO)$_2$ is disordered around the crystallographic twofold rotation axis, which intersects the host symmetry centre. Host and guest molecules in the unit cell thus have respective site multiplicities of 4 and 8, accounting for the stated 1:2 stoichiometry (Table 1). Only the oxygen atom of the solvent molecule is located on the C_2-axis and the geometry at the sulfur atom is slightly pyramidal, as usually observed.

As for the inclusion compound **3a**·(DMSO)$_5$, the TGA profile for **3b**·(DMSO)$_2$ is readily explained on the basis of its crystal structure. In contrast to the former compound, there is a one-step mass loss in TGA for **3b**·(DMSO)$_2$, which is consistent with the DMSO molecules occupying only one type of crystallographic site. It is evident from the partial packing diagram shown in Fig. 9 that each solvent molecule is accommodated within the V-shaped cleft of a host molecule and is further entrapped by methoxynaphthalene rings of neighbouring host molecules. Fig. 9 shows the complete encapsulation of two DMSO molecules that are related by the fourfold inversion centre situated at 1/2, 3/4, 5/8. As revealed by comparative space-filling diagrams, this DMSO inclusion mode is even more severely constricting than that shown in Fig. 6 and thus accounts for the exceptionally high onset temperature of desolvation (237 °C) when crystals of **3b**·(DMSO)$_2$ are heated (Table 1).

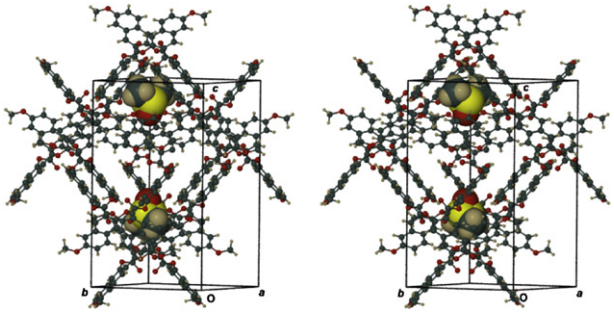

Fig. 9. Stereoview showing isolated DMSO molecules encapsulated by the host matrix in the inclusion compound **3b**·(DMSO)$_2$.

In summary, in addition to the synthesis of the novel hosts described in this paper and investigation of their inclusion properties, X-ray analyses of representative inclusion compounds of host molecules **3a** and **3b** with the common solvent DMSO revealed significant differences in host conformations as well as significantly different modes of guest inclusion. Furthermore, the X-ray structural data enabled the authors to rationalize the distinctly different thermal desolvation profiles of **3a**·(DMSO)$_5$ and **3b**·(DMSO)$_2$.

3. Experimental

3.1. General

^{1}H NMR spectra were recorded in $CDCl_3$ on a JEOL JNM-GSX 400 FT-NMR spectrometer. IR spectra were recorded with a JASCO FT-IR 4100 spectrometer. Thermogravimetric analyses (TG) were performed on a Rigaku TG-8120 instrument. X-ray analyses are described in Section 3.3. ESI mass spectra were obtained by a triple quadrupole mass spectrometer TSQ (ThermoFisher) in a positive ion mode. The capillary temperature was 250 °C, spray voltage 4.5 kV, auxiliary gas pressure 20 psi and sheath gas pressure 60 psi.

3.2. Synthesis of host compounds

*3.2.1. Synthesis of tetranaphthalide **3a**.* A mixture of 3-hydroxy-2-naphthoic acid **5** (2.8 g, 15 mmol), $POCl_3$ (3 mL, 30 mmol) and toluene (30 mL) was heated under reflux for 6 h. After cooling the reaction mixture to room temperature, water was added. The crystals deposited were separated by filtration and washed with water and aq $NaHCO_3$ solution. The crystalline solid was purified by silica gel column chromatography using AcOEt as eluent to give **3a** as white solid. Yield 54% (1.5 g); mp>300 °C; IR (Nujol) 1745 cm^{-1} (C═O); ^1H NMR ($CDCl_3$, 400 MHz) δ 8.98 (s, 4H, Ar), 7.93 (d, J=8.0 Hz, 4H, Ar), 7.76 (d, J=8.0 Hz, 4H, Ar), 7.66 (s, 4H, Ar), 7.55 (t, J=6.8 Hz, 4H, Ar), 7.48 (t, J=6.8 Hz, 4H, Ar); ^{13}C NMR ($CDCl_3$, 67.8 MHz) δ 163.5, 147.1, 136.1, 135.2, 130.8, 129.25, 129.29, 127.2, 126.7, 121.7, 120.8. Anal. Calcd for $C_{44}H_{24}O_8$: C 77.64, H 3.55; found: C 77.35, H 3.71; MS (ESI) m/z: 687.29 [M+Li]; 719.29 [M+K].

*3.2.2. Synthesis of tetranaphthalide **3b**.* A mixture of 3-hydroxy-2-naphthoic acid **5** (3.3 g, 15 mmol), $POCl_3$ (3 mL, 30 mmol) and toluene (40 mL) was heated under reflux for 6 h. After cooling the reaction mixture to room temperature, water was added. The crystals deposited were separated by filtration and washed with water and aq $NaHCO_3$ solution. The crystalline solid was purified by silica gel column chromatography using AcOEt as eluent to give **3b** as pale yellow solid. Yield 48% (1.5 g); mp>300 °C; IR (Nujol) 1742 cm^{-1} (C═O); ^1H NMR ($CDCl_3$, 400 MHz) δ 8.12 (d, J=8.8 Hz, 4H, Ar), 7.98–7.73 (m, 12H, Ar), 7.60–7.51 (m, 8H, Ar); ^{13}C NMR ($CDCl_3$, 67.8 MHz) δ 162.9, 157.9, 144.6, 132.7, 131.7, 130.9, 128.7, 122.3, 121.4, 121.0, 107.3, 55.4. Anal. Calcd for $C_{48}H_{32}O_{12}$: C 72.00, H 4.03; found: C 71.72, H 4.09; MS (ESI) m/z: 807.32 [M+Li]; 839.41 [M+K].

*3.2.3. Synthesis of tetranaphthalide **4**.* A mixture of 1-hydroxy-2-naphthoic acid **5** (2.8 g, 15 mmol), $POCl_3$ (3 mL, 30 mmol) and toluene (30 mL) was heated under reflux for 6 h. After cooling the reaction mixture to room temperature, water was added. The crystals deposited were separated by filtration and washed with water and aq $NaHCO_3$ solution. The crystalline solid was purified by silica gel column chromatography using AcOEt as eluent to give **4** as white solid. Yield 23% (0.7 g); mp>300 °C; IR (Nujol) 1731 cm^{-1} (C═O); ^1H NMR ($CDCl_3$, 400 MHz) δ 8.87 (s, 4H, Ar), 7.91 (d, J=8.8 Hz, 4H, Ar), 7.86 (s, 4H, Ar), 7.65 (s, 4H, Ar), 7.35 (d, J=8.8 Hz, 4H, Ar); ^{13}C NMR ($CDCl_3$, 67.8 MHz) δ 164.5, 148.9, 137.2, 129.3, 127.8, 127.7, 127.4, 127.2, 126.5, 123.4, 117.7. Anal. Calcd for $C_{44}H_{24}O_8$: C 77.64, H 3.55; found: C 77.38, H 3.74; MS (ESI) m/z: 687.26 [M+Li]; 719.35 [M+K].

3.3. X-ray structure determinations

X-ray diffraction data for **3a**·$(DMSO)_5$ were collected on a Nonius Kappa CCD diffractometer while those for **3b**·$(DMSO)_2$ were collected on a Bruker Apex Duo diffractometer. The crystal specimens were cooled to their respective low temperatures in a constant stream of nitrogen vapour. Unit cell refinements and data reductions were performed with DENZO-SMN[11] and SAINT+.[12] Absorption corrections were applied to both data sets.[13] Structures were solved by direct methods and refined by full-matrix least-squares methods using programs in the SHELX suite.[14] All non-H atoms were refined anisotropically. Hydrogen atoms were located in difference electron density maps and were included in a riding model with isotropic displacement parameters fixed at 1.2–1.5 those of their parent atoms.

Acknowledgements

This work was supported by 'High-Tech Research Center' Project for Private Universities: mating fund subsidy from MEXT (Ministry of Education, Culture, Sports, Science and Technology), 2005–2009. M.R.C. thanks the University of Cape Town and the NRF (Pretoria) for research support.

Supplementary data

CCDC 809198 and 802802 contain the supplementary crystallographic data for this paper. These data can be obtained free of charge at 'http://www.ccdc.cam.ac.uk/conts/retrieving.html' [or from the Cambridge Crystallographic Data Centre, 12, Union Road, Cambridge CB2 1EZ, UK; e-mail: deposit@ccdc.cam.sc.uk].

References and notes

1. *Inclusion Compounds*; Atwood, J. L., Davies, J. E. D., MacNicol, D. D., Eds.; Academic: Oxford, 1994; Vols. 1–3; *Comprehensive Supramolecular Chemistry*; Atwood, J. L., Davies, J. E. D., MacNicol, D. D., Eds.; Pergamon: Oxford, 1996; Vols. 1–11; *Separations and Reactions in Organic Supramolecular Chemistry*; Toda, F., Bishop, R., Eds.; Wiley: Chichester, 2004; Tanaka, K.; Nakashima, A.; Shimada, Y.; Scott, J. L. *Eur. J. Org. Chem.* **2006**, 2423–2428; Yun Hang, H.; Eli, R. *Angew. Chem., Int. Ed.* **2006**, *45*, 2011–2013; Scott, J. L.; Hachiken, S.; Tanaka, K. *Cryst. Growth Des.* **2008**, *8*, 2447–2452.
2. For example Tanaka, K.; Takenaka, H.; Caira, M. R. *Tetrahedron: Asymmetry* **2006**, *17*, 2216–2219; Miyata, M.; Tohnai, N.; Hisaki, I. *Acc. Chem. Res.* **2007**, *40*, 649–702; Urbanczyk-Lipkowska, Z.; Fukuda, N.; Tanaka, K. *Tetrahedron: Asymmetry* **2007**, *18*, 1254–1256.
3. Toda, F. *Acc. Chem. Res.* **1995**, *28*, 480–486; Tanaka, K.; Toda, F. *Chem. Rev.* **2000**, *100*, 1025–1074; *Organic Solid State Reactions*; Toda, F., Ed.; Kluwer: Dordrecht, 2001; *Organic Solid State Reactions, Topics in Current Chemistry 254*; Toda, F., Ed.; Springer: Berlin, 2005; MacGillivray, L. R.; Papaefstathiou, G. S.; Friscic, T.; Hamilton, T. D.; Bucar, D.-K.; Chu, Q.; Varshney, D. B.; Georgiev, I. G. *Acc. Chem. Res.* **2008**, *41*, 280–291; MacGillivray, L. R. In *Strategies and Tactics in Organic Synthesis*; Harmata, M., Ed.; Elsevier: Academic, London, 2008; pp 368–382.
4. Dickert, F.; Haunschild, A. *Adv. Mater.* **1993**, *5*, 887–895; Meinhold, D.; Seichter, W.; Kohnke, K.; Seidel, J.; Weber, E. *Adv. Mater.* **1997**, *9*, 958–961; Pirondini, L.; Dalcanale, E. *Chem. Soc. Rev.* **2007**, 695–706.
5. Gutsche, C. D. In *Calixarenes*; Stoddart, J. F., Ed.; Royal Society of Chemistry: Cambridge, 1989; *Calixarenes 2001*; Asfari, Z., Bohmer, V., Harrowfield, J., Vicens, J., Saadioui, M., Eds.; Kluwer: Dordrecht, 2001.
6. Chen, Y.; De-Xian, W.; Zhi-Tang, H.; Mei-Xiang, W. *J. Org. Chem.* **2010**, *75*, 3786–3796.
7. Morohashi, N.; Narumi, F.; Iki, N.; Hattori, T.; Miyano, S. *Chem. Rev.* **2006**, *106*, 5291–5316.
8. Tue, H.; Ishibashi, K.; Tokita, S.; Takahashi, H.; Matsui, K.; Tamura, R. *Chem.—Eur. J.* **2008**, *14*, 6125–6134.
9. Gong, B. *Chem.—Eur. J.* **2001**, *7*, 4336–4342; Gong, B. *Acc. Chem. Res.* **2008**, *41*, 1376–1386.
10. Tanaka, K.; Hayashi, S.; Caira, M. R. *Org. Lett.* **2008**, *10*, 2119–2122.
11. Otwinowski, Z.; Minor, W. *Methods Enzymol.* **1997**, *276*, 307–326.
12. *Bruker, SAINT+. Version 7.12*; Bruker AXS: Madison, Wisconsin, USA, 2008.
13. *Program SADABS, Version 2.05*; University of Göttingen: Germany, 1997.
14. Sheldrick, G. M. *Acta Crystallogr.* **2008**, *A64*, 112–122.